Force-Feedback Surgical Teleoperator: Controller Design and Palpation Experiments

Mohsen Mahvash, Jim Gwilliam, Rahul Agarwal, Balazs Vagvolgyi,
Li-Ming Su, David D. Yuh, and Allison M. Okamura

Laboratory for Computational Sensing and Robotics
Johns Hopkins University

ABSTRACT

In this paper, we develop and test a 6-degree-of-freedom surgical teleoperator that has four possible modes of operation: (1) direct force feedback, (2) graphical force feedback, (3) direct and graphical force feedback together, and (4) no force feedback. In all cases, visual feedback of the environment is provided via a head-mounted display. A position-position controller with local dynamic compensators provides the direct force feedback. The graphical force feedback is overlaid on the environment image, and displays a bar whose height and color is related to the environment force estimated using the current applied to the actuators of the patient-side arm. We evaluate the performance of the teleoperator modes in assisting a user to find the location of stiff objects hidden inside a soft material, similar to a calcified artery hidden in heart tissue and a tumor in the prostate. Seven people used the teleoperator to perform palpation in these materials. Results showed that direct force feedback mode minimizes palpation task error for the heart model.

KEYWORDS: force feedback, haptics, transparency, stability, friction compensation, observer, augmented reality.

1 Introduction

The lack of haptic feedback is often reported by surgeons to be a major limitation to current surgical teleoperators [1]. In this paper, we consider the force, or kinesthetic, component of haptics. The potential role of force feedback in assisting a surgeon can be considered for two task categories: perceptual tasks, such as palpation, and manipulation tasks, such as suturing. During perceptual tasks, haptic feedback presents the surgeon with information: the level of force applied to the surgical environment. This can help the surgeon minimize applied force and understand the material properties of the environment [2]. During a manipulation task, force feedback can physically assist the surgeon to perform the surgical task with efficient motions and in less time than without force feedback [3].

Transparency is the most common measure used to evaluate the performance of a force-feedback teleoperator [4]. An ideal transparent teleoperator transmits both the exact forces and the exact impedance of the teleoperated environment to the operator. It is hypothesized that the transparency of a teleoperator is the main factor that determines whether force feedback is useful for performing a perceptual task. Transparency can be compromised when a position-position controller is used in lieu of force sensors, due to undesirable dynamic properties of the teleoperator. Consider a force feedback teleoperator that transmits the both the friction forces from the joints of the robot arms and the environment force to the human operator. If the friction force of the arms is the same as or greater than the environment force, the friction force will mask the environment force and therefore the force feedback will not give useful information about the environment properties to the operator.

Developing highly transparent force feedback for a surgical teleoperator is challenging because (1) the use of force sensor on the patient-side arm is limited for practical reasons, (2) the dynamic force of the arms of a surgical teleoperator is generally in the scale of the environment force, (3) link flexibility and the tendon elasticity reduce transparency, and (4) the trade-off between the transparency and stability of a teleoperator limit the controller performance [5][6].

In this paper, we explain the components of a surgical teleoperator that can operate in four possible modes of operation: (1) direct force feedback, (2) graphical force feedback, (3) direct and graphical force feedback together, and (4) no force feedback. We use a position-position controller with local compensators to provide direct force feedback without using force sensors. The performance of the teleoperator in different modes is evaluated in performing two sets of palpation tasks. The palpated environment for the first task is designed to be similar to heart tissue with a calcified artery, and for the second task, similar to a prostate tissue with a cancerous tumor inside. The details of controller can be found in prior publications [5][6]; this paper focuses on the system structure and evaluation.

The remainder of the paper is organized as follows: Section 2 describes the teleoperator system, including its position-position controller, local compensators, and the force observer used for graphical force feedback. Section 3 explains the palpation experiments and the results of performing the task in the four different feedback modes. Section 4 summarizes the conclusions and provides considerations for future work.

2 Teleoperator System

The teleoperator system contains one master manipulator and one patient-side manipulator of the da Vinci surgical system [7][8] (Figure 1) provided by Intuitive Surgical, Inc., and a custom control system developed at the Johns Hopkins University [5][6].

This work was performed at the Johns Hopkins University Laboratory for Computational Sensing and Robotics, 3400 N. Charles Street, Baltimore, MD 21218. The contact author email is aokamura@jhu.edu. L. Su and D. D. Yuh are surgeons with the Johns Hopkins Medical Institutions. M. Mahvash is now with Boston University.

This work was supported by National Science Foundation grants IIS-0347464 and EEC-9731748 and National Institutes of Health grant #R01 EB002004. The authors thank P. Kazanzides, A. Kapoor, C. Reiley, I. Iordachita, and L. Verner of JHU, and Christopher Hasser of Intuitive Surgical, Inc. for their contributions to the experiment design and setup.

Symposium on Haptic Interfaces for Virtual Environments and Teleoperator Systems 2008
13-14 March, Reno, Nevada, USA
978-1-4244-2005-6/08/$25.00 ©2008 IEEE

(a)

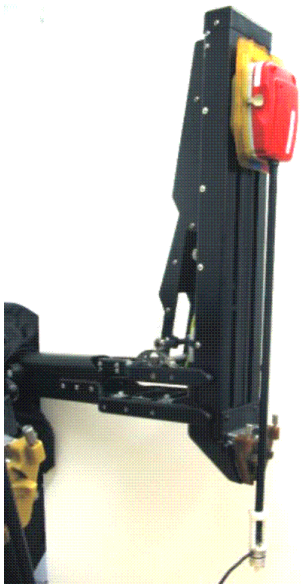

(b)

Figure 1. (a) Master manipulator and (b) patient-side manipulator of a custom version of the da Vinci surgical system assembled at Johns Hopkins University.

2.1 Control System

The custom control system contains proportional tracking controllers, friction compensators, and inertia compensators.

The transparency of the teleoperator in transmitting the stiffness of the environment to the user depends on the stiffness of the environment. The controllers perform as a network of virtual springs that connects the tip of the slave and master manipulator to each other (Figure 2).

This way, assuming that the inertia and friction of the master and slave manipulators are zero and the links of the manipulators are extremely rigid, the transmitted impedance to the user along each axis is

$$z = \frac{rk}{r+k}, \tag{1}$$

where r is the impedance of the environment and k is the gain of proportional controllers (or stiffness of the virtual springs). The teleoperator is transparent for very soft environments, such that $r << k$. Lack of a force sensor inherently limits the transparency of such a teleoperator [4][5].

Local controllers are used to cancel the inertia and Coulomb friction of the arms (Figure 2). Local controllers contain friction compensators and inertia compensators, which are explained in the following sections.

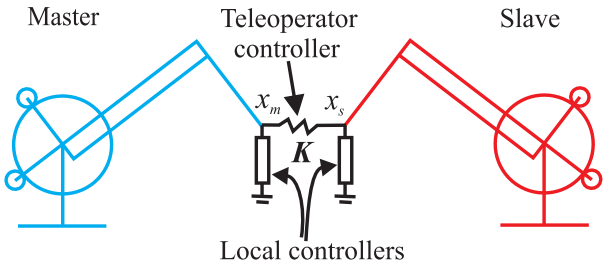

Figure 2. The proportional tracking controllers connect the tips of the slave manipulator to the master manipulator. Local controllers cancel friction and inertia of the manipulators.

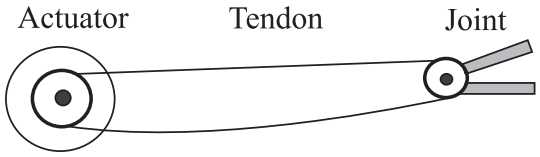

Figure 3. A tendon-driven joint. Friction occurs in all stages of the tendon-driven joint, including the actuator and the remote joint.

2.1.1 Friction Compensator

Friction compensation is performed in the joints of the slave manipulator. We use a single-elastic friction compensator for each tendon-driven joint to cancel Coulomb friction [6]. Friction occurs at several stages of the joint, including the actuator that moves the tendon, the joint of the manipulator driven by the tendon, and the pulleys that support the tendon (Figure 3). The single state friction compensator provides full compensation when all stages of the tendon-driven joint moves in the same direction, but it does not provide full friction compensation when the user changes the direction of the motion of the joint.

2.1.2 Inertia Compensator

Inertia compensation is performed in the joint space of the slave manipulator. The compensator for each joint includes a feedforward term that estimates the reflected inertia of the arm to that joint. The reflected inertia at each joint is calculated by the acceleration of the joint multiplied by the effective mass of the joint. The effective mass of each joint depends on configuration of the arm. The controller cancels 90% of the minimum effective mass for each joint at low frequencies [5].

The velocity and acceleration of the joints are calculated by the first and second derivatives of the positions of the joints of the arm and then are filtered by first- and second-order low-pass filters to remove encoder noise. These filters also limit the effects of high-frequency unmodeled dynamics due to transmission cables of the manipulators from being excited. The inertia compensation is performed at low frequencies due to low pass filters.

2.1.3 System Performance

The transparency of teleoperator was evaluated during two tests. During the first test, the slave arm deflects a piece of foam. During the second test, the slave stretched a rubber band several times [5][6]. Figure 4 and Figure 5 show that the friction and inertia compensation significantly improve the transparency of the teleoperator. In these figures, the forces transmitted to the operator closely approximate the forces measured by a force sensor when the compensation algorithms are used.

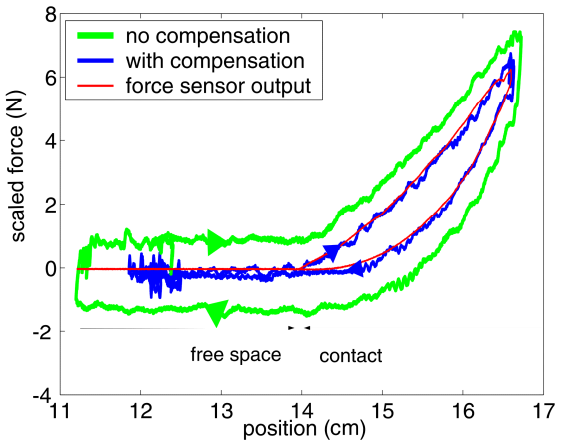

Figure 4. Force-displacement curves of the teleoperator during probing of a soft object with and without friction compensation.

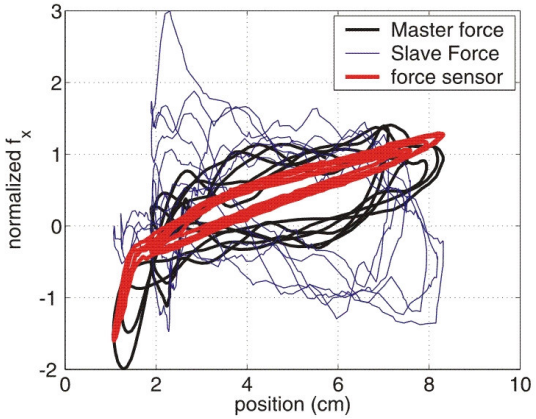

Figure 5. Force-displacement curves during stretching of a rubber for several cycles when friction and inertia of the slave manipulator are compensated. The master force shows the force of the teleoperator when inertia is compensated.

2.2 Graphical Force Feedback

Force information is displayed graphically on the vision channel, providing a form of sensory substitution. Figure 6a shows a user wearing a head-mounted display (HMD) sitting at the master console, and Figure 6b shows the image seen by the user from one of the two eyepieces.

2.2.1 Force Estimation

The graphical force feedback is overlaid on the environment image, and displays a bar whose height and color is related to the environment force estimated by an observer using the current applied to the actuators of the patient-side arm. A state observer is used to estimate environment force, using the method of [9]. The force displayed on the HMD can be a better match than the force applied through direct force feedback, since visual displays alone will not affect the stability of the system. In the case of direct feedback, we are limited to force feedback that maintains stability.

2.2.2 Instrument Tracking and Force Display

The visualization engine of the display system is based on the Surgical Assistance Workstation software architecture [10]. It is

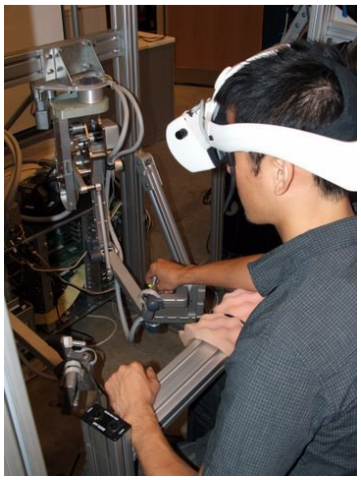

(a)

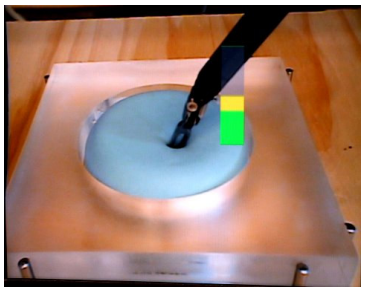

(b)

Figure 6. The vision system that displays the force information. (a) a user wears a head-mount display, (b) The image of the environment, overlaid with a bar that changes height and color depending on the level of applied force.

capable of simultaneous capture, computation, and visualization of multiple data streams running on a computer workstation. The video processing pipeline consists of the following elements: stereo video capture, stereo rectification, conversion to OpenGL texture, generating visual overlay texture, information fusion, OpenGL 3D rendering.

As a prerequisite, the stereo camera system is carefully calibrated and the calibration results (intrinsic and extrinsic camera parameters) are fed to the rectification algorithm and the 3D visualization system. Thus, the stereo images rendered in the head-mounted display are perfectly aligned and it is possible to position the graphical overlay accurately in the virtual 3D space. In addition, we determined the position of the robot's 3D frame in camera coordinates in order to make transformation between the two coordinate systems possible.

During operation, the display system connects to the robot control software via TCP/IP and acquires the live force values and robot tool-tip positions computed from the joint kinematics. Then it converts the tool-tip coordinates to camera coordinates and places the overlay to that position. The color-coded graphic overlay is generated according to the latest force values, and the system renders the overlay on top of the rectified live camera images. As a result, in the stereo head mounted display the graphical overlay appears to be in the same 3D position as the tool tip.

Our experiments suggest that the graphical overlay corresponding to a certain visual feature on the image (in our case the tool tip) shall be rendered in the same stereo disparity (i.e.

perceived distance) as the corresponding visual feature. Otherwise, the continuous switching between the two different disparities puts unnecessary stress on the human eye.

3 Human-Subject Experiments

The purpose of this experiment is to evaluate the benefits of direct force feedback and graphical force feedback on user performance during two palpation tasks applicable to surgery.

3.1 Methods

3.1.1 Participants

Seven right-handed subjects were asked to perform two palpation tasks with our custom version of the da Vinci Surgical System, using all four of the feedback modes described earlier. Only one of the users had previous experience with the system and most users had little to no experience with haptic feedback in virtual or teleoperated environments. The users were not medical professionals.

3.1.2 Heart and Prostate Models

The experiment consisted of two tasks: (1) palpation of synthetic heart models to locate and determine the orientation of an embedded plastic stick (a coffee stir straw) in each model, and (2) palpation of synthetic prostate models to locate the position of a hardened nodule under the surface of each model.

Heart and prostate models were both cast using the silicon rubber compound OOMOO 25 (Smooth-On, Easton, PA). Heart models were mixed at a ratio of 4:1::B:A, while prostate models were cast at a ratio of 1:1::B:A. Each heart model contained a coffee straw inserted through the center of the model horizontally at a depth of approximately 8-10 mm from the top surface (Figure 7). Each prostate model contained a nodule (~1 cm diameter) under the surface of the model in one of six distinct locations (Figure 8).

3.1.3 Experimental Procedure

All trials were performed with subjects using the right arm of the master manipulator to palpate the model. The subjects viewed the environment through a head mounted display (HMD), as shown in Figure 6a. The particular palpation technique was left to the discretion of the subject. The most common techniques involved palpation of the model with the tool tip (needle driver) perpendicular to the surface or dragging the tool tip across the surface of the model (Figure 9).

For both tasks, each of the following four separate feedback conditions were distributed equally and pseudo-randomly among the twelve trials: (1) direct force feedback, (2) graphical force feedback, (3) direct and graphical force feedback together, and (4) no force feedback. The direct force feedback used the position-position controller and dynamic compensators described in Section 2.1. The graphical force feedback consisted of a bar that changed height and to displayed tool tip forces during palpation, overlaid on the image of the environment as described in Section 2.2 and shown in Figure 6b. The two tasks described below, the "heart" task and the "prostate" task, were performed in random order by each subject.

Prior to the "heart" task, subjects were allowed to feel an example heart model, and were instructed to detect the coffee straw and its orientation by hand. Each of the twelve heart models contained an embedded straw that was oriented randomly between four angles measuring (0, 45, 90, 135) degrees from the horizontal. The four orientation angles were distributed equally among the twelve trials. Subjects were then allowed to practice

Figure 7. A heart model that contains a plastic stick (a coffee stir straw) inserted through its center.

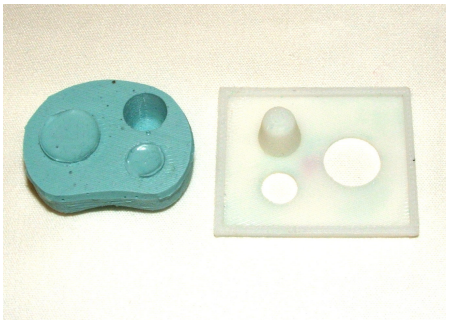

(a)

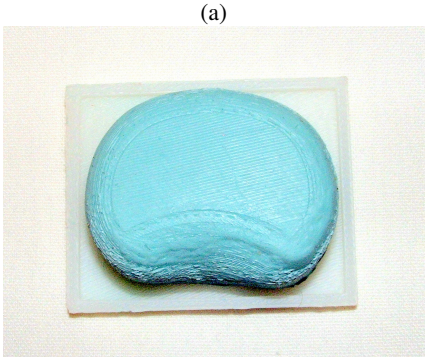

(b)

Figure 8. A prostate model that contains a nodule. (a) The prostate "tissue" is shown from the underside, which is mated with the fuse-deposition-manufactured base and nodule. (b) The view of the prostate model seen by the user.

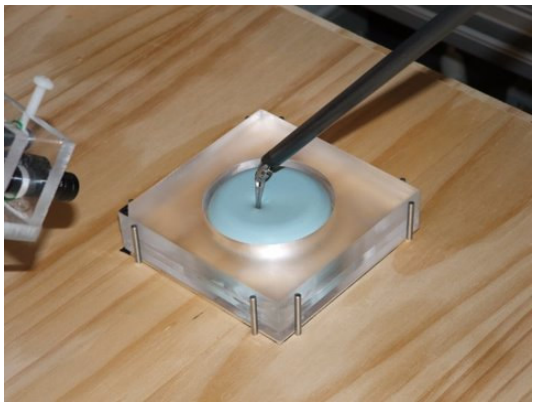

Figure 9. A user palpates the heart model using a da Vinci instrument. The model is fixed to the table, so it does not move during haptic exploration.

palpating the heart model with the da Vinci system using all four feedback conditions. After being familiarized with the feedback conditions, each trial consisted of the following steps: (1) the subject was instructed to palpate the heart model, as shown in Figure 9, and identify the orientation of the embedded artery (plastic coffee stir straw) as closely as possible. (2) Once the subject believed that he or she had correctly determined the straw orientation, the subject verbally notified the experiment administrator, at which time recording of force and position data stopped. (3) The experiment administrator, who was blinded to the actual orientation of the embedded straw, placed a stir straw on top of the model at the 0° orientation and rotated it either clockwise or counter clockwise based on the subject's verbal instructions. (4) When the subject was satisfied with the orientation of the straw, an overhead picture was then taken for accuracy analysis. Steps 1-4 were repeated for all twelve trials.

Prior to the "prostate" task, subjects were allowed to feel an example prostate model. They were instructed to detect the nodule and its location by hand. They were then familiarized with all four feedback conditions of the system using the same practice model. Models were assigned pseudo-randomly to each of twelve trials (ensuring that each of twelve models was used in one trial), which effectively randomized nodule location. Each trial consisted of two steps: (1) the subject was instructed to palpate the prostate model and identify the location of the nodule. (2) Once the subject believed that he or she had identified the correct location of the nodule, the subject held the tool-tip at that location, and an overhead digital photograph was taken for accuracy analysis. Steps 1 and 2 were repeated for all twelve trials. After all trials were completed, an experiment administrator analyzed the digital photographs to determine whether the subject was pointing to a location within 1 cm of the center of the actual nodule. This evaluation was performed with the experimenter blinded to the feedback condition.

The tasks required significant concentration and the entire experiment took each subject between one and two hours to complete, with short (1- to 5-minute) breaks between each trial and a long (10- to 15-minute) break between tasks. For all trials, the image seen through the HMD was recorded for the duration of the trial. Additionally, the tool tip forces and positions were recorded throughout each trial.

3.2 Results and Discussion

Figure 10 and Figure 11 show the accuracy of subjects' identification of the artery (for the heart) and the nodule (for the prostate), respectively. The results of the heart model shows that direct force feedback allows for more accurate identification of the stiff regions of the objects compared to no feedback or graphical feedback alone. However, prostate tests show that there is no significant difference in the average accuracy of most modes of the teleoperator.

To further investigate the results, we used one-tailed t-test to compare accuracy averages of each pair modes of teleoperation. We assigned 1 to a successful trail and 0 to unsuccessful one. There are 21 numbers including 0 and 1 for each mode of teleoperation. Table 1 and Table 2 show the hypotheses tested for each pair of data and the *p*-values of the t-tests. We define that there is a significant statistical evidence for a hypothesis to be true when its *p*-value is smaller than 0.05 and there is no significant evidence for a hypothesis when its *p*-value is larger than 0.05.

The results of Table 1 show that there is significant evidence that direct force feedback provides the user with more accurate identification for heart model than either no feedback or graphical force feedback. The results also show that the no force feedback

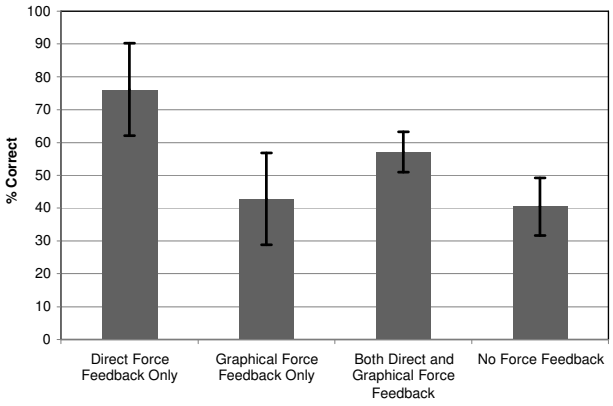

Figure 10. Accuracy of finding the correct nodule location in the heart model. Data is averaged over all seven subjects, and standard error bars are shown.

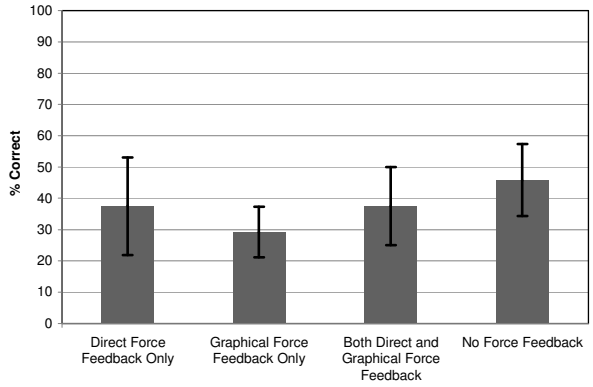

Figure 11. Accuracy of finding the correct nodule location in the prostate model. Data is averaged over all seven subjects, and standard error bars are shown.

mode provides more accurate identification than graphical force feedback for prostate model. There is no significant evidence for other hypotheses listed in Table 1 and Table 2. (In these tables, "<" and ">" mean "worse than" and "better than", respectively. In Figure 10 and Figure 11, a taller bar is better and a shorter bar is worse.)

To physically investigate the results, we displayed the force-deflection responses of the models transmitted to the user. Figure 12 and Figure 13 compare force deflection of the heart and prostate models on and near the hard inclusions. There is significant difference between the stiffness of the two places for the heart model, but not for the prostate model. The study in [2] shows that a user can detect a 23% change in stiffness. The change of the stiffness in heart model is about 100%. The teleoperator is sufficiently transparent for the heart models. There is no considerable difference between the stiffness of the prostate model at and near hard object, as shown in Table 2. The teleoperator is not transparent for prostate models because they are very stiff. The user cannot detect the hard object due to imperfect information sent by the teleoperator to the user. However, the teleoperator alone may not be to blame, since even using a hand-held stylus to directly palpate the prostate and detect the nodule is difficult. Through informal experiments, we found that the nodule could be much more easily detected using bare hand palpation rather than a stylus. Since the difference between

Table 1. Hypotheses and *p*-values of t-tests for heart models.

Hypothesis (Heart)	*p*-value	Significant?
direct only > graphical only	0.0077	Yes
direct only > direct and graphical	0.0811	No
direct only > no feedback	0.0038	Yes
graphical only < direct and graphical	0.1646	No
graphical only > no feedback	0.3328	No
direct and graphical > no feedback	0.0517	No

Table 2. Hypotheses and *p*-values of t-tests for prostate models.

Hypothesis (Prostate)	*p*-value	Significant?
direct only > graphical only	0.1334	No
direct only > direct and graphical	0.3557	No
direct only < no feedback	0.3328	No
graphical only < direct and graphical	0.2464	No
graphical only < no feedback	0.0211	Yes
direct and graphical < no feedback	0.2464	No

the prostate nodule stiffness and the surrounding soft tissue stiffness is so little, a tactile sensor and display may be more appropriate for this case of haptic exploration [11].

In these experiments, it appears that the graphical force display either confused the users or distracted their attention from other modes of force feedback, including natural information about material deflection that is visible in the image of the environment. The negative results for graphical display in this experiment may appear to contradict previous studies by our group using a clinical da Vinci Surgical System with and without graphical display [12][13]. However, there are many differences between the present experiment and the previous work: the visual display medium, the form of the graphical feedback, and the nature of the task. First, in the present work, an HMD was used on a custom da Vinci system, to allow direct comparison between direct and graphical force feedback. In the previous work, the high-resolution CRTs that are a part of the commercially available da Vinci were used. Second, the graphical display in the present work was a bar graph that changed color and size with the level of estimated force. The previous work used strain gage sensors mounted on the da Vinci instruments, so only bending forces were measured. In addition, the graphical display consisted of a small dot, overlaid on the top if the instrument, which changed only color. Third, the task in the previous experiments was suture knot-tying, which is a manipulation task and may have different haptic-feedback requirements from the palpation/exploration tasks considered here. In addition, there was a very low level of direct force feedback that is provided by the commercially available da Vinci system, and this was available in both graphical force feedback and no force feedback conditions.

4 Conclusions

This paper presents a surgical teleoperator with direct force feedback and graphical force feedback. The force feedback is provided with a position-position controller with friction and inertia compensation, and the graphical feedback is provided by augmenting the visual display with a graphical representation of the applied force. Seven subjects used the teleoperator to palpate prostate and heart models that contained hard inclusions. Results show that the users are able of finding the location of hard objects when the teleoperator is sufficiently transparent. In future work specific to this paper, we will improve the graphical/visual force feedback by using CRTs rather than an HMD to display the

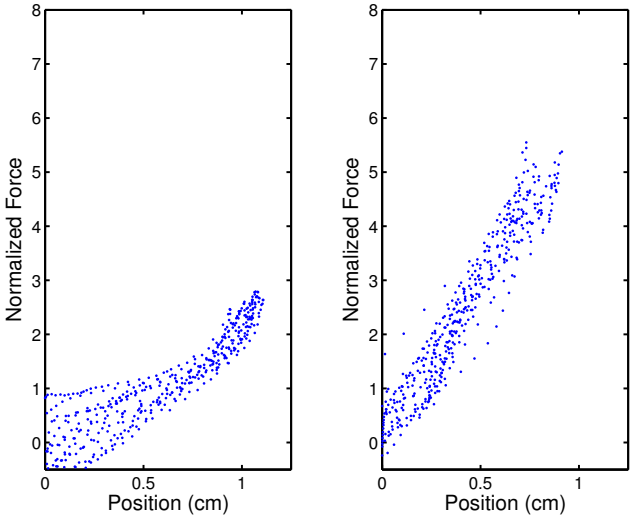

Figure 12. Force-deflection response for a heart model near (left) and on (right) a hard inclusion.

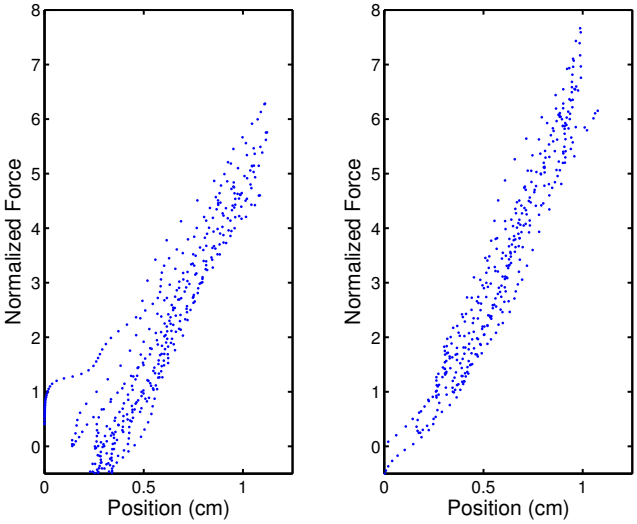

Figure 13. Force-deflection response for a prostate model near (left) and on (right) a hard inclusion.

graphics. In addition, we plan to run trials with surgeon subjects who are both novices and experts with clinical use of the da Vinci surgical system.

More broadly, while great strides have been made toward applying force feedback in robot-assisted minimally invasive surgery, there is still no clinically practical system that can both provide useful force display and a high level of dexterity at the instrument tips [14]. The primary difficulty appears to be in force sensing and estimation, not display, although stability issues often couple the two problems. Force sensors are currently incompatible with surgical environments for most existing robotic systems, both in clinical practice and in research, although promising integrated devices are being developed [15].

One promising area for future work is the use of the surgical system's visual channel for deformation measurement and tissue property acquisition. Visually sensed deformation, with or without force sensing, may also be used in tissue parameter estimation. If intra-operative tissue models can be developed quickly, force display could be based on the model rather than the current

estimated force. Such model-based teleoperation could be particularly useful in the presence of large time delays. (Although a significant body work has addressed methods for maintaining teleoperator stability with time delays, force feedback in conditions where the delay is large is inherently poor and difficult to use – even if the system remains stable.)

In addition, while experiments have demonstrated the usefulness of force feedback in specific contexts, there is little fundamental understanding of *why* force feedback is useful in surgical procedures, other than the work of Wagner and Howe [3]. The use of tactile information in surgery, using methods such as those in [11], and the possibility of using force feedback in fewer degrees of freedom to facilitate force sensor integration [16], should also be further explored.

Finally, training with robot-assisted surgical systems could also benefit from haptic feedback, even if the feedback is not implemented in actual surgeries. Surgeons currently perform satisfactorily by observing tissue deformation and using internal models of tissue properties to estimate the applied force. Yet this requires the surgeon to have an accurate model of the tissue's force-deformation relationship, presumably acquired through previous. Thus, haptic feedback may prove to be useful for surgeon training with robotic systems on phantom or animal models. In such environments, it may be possible to use force sensors, since the practical constraints are not as stringent.

References

[1] F. W. Mohr, V. Falk, A. Diegeler, T. Walther, J. F. Gummert, J. Bucerius, S. Jacobs, and R. Autschbach. Computer-enhanced "robotic" heart surgery: Experience in 148 patients. *Journal of Thoracic and Cardiovascular Surgery*, 121(5):842–853, 2001.

[2] Jones, L. A. and Hunter, I. W. 1990. A perceptual analysis of stiffness. *Experimental Brain Research*. 79, 150—156, 1990.

[3] C. R. Wagner, N. Stylopoulos, P. G. Jackson, and R. D. Howe. The Benefit of Force Feedback in Surgery: Examination of Blunt Dissection. *Presence: Teleoperators and Virtual Environments.* 16(3): 252-262, 2007.

[4] D. A. Lawrence. Stability and transparency in bilateral teleoperation. *IEEE Transactions on Robotics and Automation*, 9(5):624–637, 1993.

[5] M. Mahvash and A. M. Okamura. Enhancing transparency of a position exchange teleoperator. In *Second Joint Eurohaptics Conference and Symposium on Haptic Interfaces for Virtual Environment and Teleoperator Systems (World Haptics),* pages 470–475, 2007.

[6] M. Mahvash and A. M. Okamura. Friction compensation for enhancing transparency of a teleoperator with compliant transmission. IEEE Transactions on Robotics, 23(6):1240–1246, 2007.

[7] Intuitive Surgical, Inc. http://www.intuitivesurgical.com/. Last accessed December 1, 2007.

[8] G. Guthart and J. K. Salisbury. The Intuitive Telesurgery System: Overview and application. *In IEEE Int. Conf. Rob. Aut*., pages 618–621, 2000.

[9] P. J. Hacksel and S. E. Salcudean "Estimation of environmental forces and rigid body velocities using observers." In *IEEE International Conference on Robotics and Automation*, pp. 931–936, 1994.

[10] Surgical Assistance Workstation website, Engineering Research Center for Computer-Integrated Surgical Systems and Technology: http://www.cisst.org/cisst/saw/. Last accessed December 1, 2007.

[11] R. D. Howe, W. J. Peine, D. A. Kontarinis, and J. S. Son. Remote palpation technology. *IEEE Engineering in Medicine and Biology* Magazine, 14(3):318–323, 1995.

[12] M. Kitagawa, D. Dokko, A. M. Okamura, and D. D. Yuh. Effect of sensory substitution on suture manipulation forces for robotic surgical systems. Journal of Thoracic and Cardiovascular Surgery, 129(1):151–158, 2005.

[13] C. E Reiley, T. Akinbiyi, D. Burschka, D. C. Chang, A. M. Okamura, and D. D. Yuh. Effects of visual force feedback on robot-assisted surgical task performance. Journal of Thoracic and Cardiovascular Surgery, 2008. In press.

[14] A. M. Okamura, L. N. Verner, C. E. Reiley, and M. Mahvash. Haptics for robot-assisted minimally invasive surgery. In *Proceedings of the International Symposium Robotics Research*, Hiroshima, Japan, November 26-29, 2007. To be published in Robotics Research: Results of the 12th International Symposium Robotics Research, Springer Tracts in Advanced Robotics.

[15] B. Kuebler, U. Seibold, and G. Hirzinger. Development of actuated and sensor integrated forceps for minimally invasive robotic surgery. International Journal of Medical Robotics and Computer Assisted Surgery, 1(3):96–107, 2005.

[16] L. N. Verner and A. M. Okamura. Sensor/actuator asymmetries in telemanipulators: Implications of partial force feedback. In *14th Symposium on Haptic Interfaces for Virtual Environment and Teleoperator Systems*, pages 309–314, 2006.